PHYSICAL REVIEW D **94,** 105011 (2016)

Instanton-dyon liquid model. III. Finite chemical potential

Yizhuang Liu,[*] Edward Shuryak,[†] and Ismail Zahed[‡]

Department of Physics and Astronomy, Stony Brook University, Stony Brook, New York 11794-3800, USA

(Received 24 June 2016; published 14 November 2016)

We discuss an extension of the instanton-dyon liquid model that includes light quarks at finite chemical potential in the center symmetric phase. We develop the model in details for the case of $SU_c(2) \times SU_f(2)$ by mapping the theory on a three-dimensional quantum effective theory. We analyze the different phases in the mean-field approximation. We extend this analysis to the general case of $SU_c(N_c) \times SU_f(N_f)$ and note that the chiral and diquark pairings are always comparable.

DOI: 10.1103/PhysRevD.94.105011

I. INTRODUCTION

This work is a continuation of our earlier studies [1,2] of the gauge topology in the confining phase of a theory with the simplest gauge group $SU(2)$. We suggested that the confining phase below the transition temperature is an "instanton dyon" (and antidyon) plasma which is dense enough to generate strong screening. The dense plasma is amenable to standard mean-field methods.

The treatment of the gauge topology near and below T_c is based on the discovery of Kraan-van-Baal-Lee-Lu (KvBLL) instantons threaded by finite holonomies [3] and their splitting into the so called instanton dyons (antidyons), also known as instanton monopoles or instanton quarks. Diakonov *et al.* [4,5] suggested that the backreaction of the dyons on the holonomy potential at low temperature may be at the origin of the order-disorder transition of the Polyakov line. Their model was based on (parts of) the one-loop determinant providing the metric of the moduli spaces in Bogomolny-Prasad-Sommerfeld (BPS)-protected sectors, purely self-dual or anti-self-dual. The dyon-antidyon interaction is not BPS protected and appears at the leading—classical—level, related with the so-called streamline configurations [6].

The dissociation of instantons into constituents was advocated by Zhitnitsky *et al.* [7]. Using controlled semi-classical techniques on $S^1 \times R^3$, Unsal and his collaborators [8] have shown that the repulsive interactions between pairs of dyon-antidyon (bions) drive the holonomy effective potential to its symmetric (confining) value.

Since the instanton dyons carry topological charge, they should have zero modes as well. On the other hand, for an arbitrary number of colors N_c, those topological charges are fractional $1/N_c$, while the number of zero modes must be integers. Therefore, only some instanton dyons may have zero modes [9]. For general N_c and a general periodicity angle of the fermions, the answer is known but a bit involved. For $SU(2)$ colors and physically antiperiodic fermions, the twisted L dyons have zero modes, while the usual M dyons do not. Preliminary studies of the dyon-antidyon vacuum in the presence of light quarks were developed in Refs. [10,11]. In supersymmetric QCD, some arguments were presented in Ref. [12].

In this work, we would like to follow up on our recent studies in Refs. [1,2] by switching a finite chemical potential in the center symmetric phase of the instanton-dyon ensemble with light quarks. We will make use of a mean-field analysis to describe the interplay of the spontaneous breaking of chiral symmetry with color superconductivity through diquark pairing. One of the chief achievements of this work is to show how the induced chiral effective Lagrangian encodes about confinement at finite μ. In particular, we detail the interplay between the spontaneous breaking of chiral symmetry, the pairing of diquarks, and center symmetry.

Many model studies of QCD at finite density have shown a competition between the pairing of quarks [13], chiral density waves [14], and crystals [15,16] at intermediate quark chemical potentials μ. We recall that for $SU_c(2)$ the diquarks are colorless baryons and massless by the extended flavor $SU_f(4)$ symmetry [13]. Most of the models lack a first principle description of center symmetry at finite chemical potential. This concept is usually parametrized through a given effective potential for the Polyakov line as in the Polyakov–Nambu–Jona-Lasinio models [17]. We recall that current and first principle lattice simulations at finite chemical potential are still plagued by the sign problem [18], with some progress on the bulk thermodynamics [19].

In Sec. II, we detail the model for two colors. By using a series of fermionization and bosonization techniques, we show how the three-dimensional effective action can be constructed to accommodate for the light quarks at finite μ. In Sec. III, we show that the equilibrium state at finite T, μ supports center symmetry but competing quark-antiquark or quark-quark pairing. In Sec. IV, we generalize the results to arbitrary colors N_c. Our conclusions are in Sec. V. In Appendix A, we briefly discuss the transition matrix in the

[*]yizhuang.liu@stonybrook.edu
[†]edward.shuryak@stonybrook.edu
[‡]ismail.zahed@stonybrook.edu

string gauge at finite μ. In Appendix B, we estimate the transition matrix element in the hedgehog gauge. In Appendix C, we recall the key steps for the bosonization and fermionization that help streamline the logic and notations used at finite μ. In Appendix D, we give an alternative but equivalent mean-field formulation with a more transparent diagrammatic content. In Appendix E, we detail the construction of the zero modes for arbitrary Matsubara frequencies.

II. EFFECTIVE ACTION WITH FERMIONS AT FINITE μ

A. General setting

In the semiclassical approximation, the Yang-Mills partition function is assumed to be dominated by an interacting ensemble of instanton dyons (antidyons). For interparticle distances large compared to their sizes—or a very dilute ensemble—both the classical interactions and the one-loop effects are Coulomb-like. At distances of the order of the particle sizes, the one-loop effects are encoded in the geometry of the moduli space of the ensemble. For multidyons, a plausible moduli space was argued starting from the KvBLL caloron [3] that has a number of pertinent symmetries, among which are permutation symmetry, overall charge neutrality, and clustering to KvBLL.

Specifically and for a fixed holonomy $A_4(\infty)/2\omega_0 = \nu\tau^3/2$ with $\omega_0 = \pi T$ and $\tau^3/2$ being the only diagonal color algebra generator, the $SU(2)$ KvBLL instanton (anti-instanton) is composed of a pair of dyons labeled by L and M (antidyons by $\overline{L}$ and $\overline{M}$) in the notations of Ref. [4]. Generically, there are $N_c - 1$ M dyons and only one twisted L dyon type. The $SU(2)$ grand-partition function is

$$\mathcal{Z}_1[T] \equiv \sum_{[K]} \prod_{i_L=1}^{K_L} \prod_{i_M=1}^{K_M} \prod_{i_{\overline{L}}=1}^{K_{\overline{L}}} \prod_{i_{\overline{M}}=1}^{K_{\overline{M}}} \times \int \frac{f_L d^3x_{Li_L}}{K_L!} \frac{f_M d^3x_{Mi_M}}{K_M!} \frac{f_L d^3y_{\overline{L}i_{\overline{L}}}}{K_{\overline{L}}!} \frac{f_M d^3y_{\overline{M}i_{\overline{M}}}}{K_{\overline{M}}!} \times \det(G[x]) \det(G[y]) |\det \tilde{\mathbf{T}}(x,y)| e^{-V_{D\overline{D}}(x-y)}. \quad (1)$$

Here, x_{mi} and y_{nj} are the three-dimensional coordinates of the i dyon of m kind and j antidyon of n kind. Here, $G[x]$ is a $(K_L + K_M)^2$ matrix, and $G[y]$ is a $(K_{\overline{L}} + K_{\overline{M}})^2$ matrix of which the explicit forms are given in Refs. [4,5]. $V_{D\overline{D}}$ is the streamline interaction between $D = L$, M dyons and $\overline{D} = \overline{L}$, $\overline{M}$ antidyons as numerically discussed in Ref. [6]. For the $SU(2)$ case, it is Coulombic asymptotically with a core at short distances [1].

The fermionic $\det \tilde{\mathbf{T}}(x,y)$ determinant at finite chemical potential will be detailed below. The fugacities f_i are related to the overall dyon density. The dyon density n_D could be extracted from lattice measurements of the caloron plus anticaloron densities at finite temperature in unquenched lattice simulations [20]. No such extractions are currently available at finite density. In many ways, the partition function for the dyon-antidyon ensemble resembles the partition function for the instanton–anti-instanton ensemble [21].

B. Quark zero modes at finite μ

At finite μ, the exact zero modes for the L dyon (right) and $\overline{L}$ antidyon (left) in the hedgehog gauge are defined as $\varphi^A_\alpha = \eta^A_\beta \epsilon_{\beta\alpha}$ with indices A for color and α for spinors. The normalizable M-dyon zero mode are periodic at finite μ. The L-dyon zero modes are antiperiodic at finite μ. At finite T, μ, they play a dominant role in the instanton-dyon model with light quarks. Keeping in the time dependence only the lowest Matsubara frequencies $\pm\omega_0$, their explicit form is

$$\eta_R = \frac{1}{2}\sum_{\xi=\pm} \alpha_\xi(r) \mathbf{S}_+ (1 - \xi\sigma\cdot\hat{r}) e^{i\xi(\omega_0 x_4 + \alpha_R)}$$
$$\eta_L = \frac{1}{2}\sum_{\xi=\pm} \alpha_\xi(r) \mathbf{S}_- (1 + \xi\sigma\cdot\hat{r}) e^{i\xi(\omega_0 x_4 + \alpha_L)} \quad (2)$$

with

$$\alpha_\pm(r) = \frac{\mathbf{C} e^{\pm i\mu r}}{\sqrt{(v_l\omega_0 r)\mathrm{sh}(v_l\omega_0 r)}} \times \left(\mp \frac{2i\mu}{v_l\omega_0} + \left(e^{\mp 2i\mu r} - \frac{2}{e^{v_l\omega_0 r} + 1} \right) \right). \quad (3)$$

$\mathbf{C}$ is an overall normalization constant, and the $SU(2)$ gauge rotation $\mathbf{S}_\pm$ satisfies

$$\mathbf{S}_\pm (\sigma\cdot\hat{r}) \mathbf{S}^\dagger_\pm = \pm\sigma_3, \quad (4)$$

translating from the hedgehog to the string gauge. In (2), $\alpha_{L,R}$ correspond to the rigid $U(1)$ gauge rotations that leave the dyon coset invariant. We have kept them as they do not drop in the hopping matrix elements below. The oscillating factors $e^{\pm 2i\mu r}$ are Friedel-type oscillations. For $\mu = 0$, we recover the zero modes in Refs. [2,10]. We have checked that the periodic M-dyon zero modes are in agreement with those obtained in Ref. [22]. The restriction to the lowest Matsubara frequencies makes the mean-field analysis reliable only for $\mu/3\omega_0 < 1$ and for temperatures in the range of the critical temperature. The instanton liquid model becomes increasingly dense as $T \to 0$, whereby our mean-field analysis becomes less reliable in general, as detailed in Refs. [1,2].

C. Fermionic determinant at finite μ

The fermionic determinant can be viewed as a sum of closed fermionic loops connecting all dyons and antidyons. Each link—or hopping—between L dyons and $\overline{L}$ antidyons is described by the elements of the "hopping chiral matrix" $\tilde{\mathbf{T}}$,

$$\tilde{\mathbf{T}}(x,y) \equiv \begin{pmatrix} 0 & i\mathbf{T}_{ij} \\ i\mathbf{T}_{ji} & 0 \end{pmatrix}, \tag{5}$$

with dimensionality $(K_L + K_{\overline{L}})^2$. Each of the entries in $\mathbf{T}_{ij}$ is a "hopping amplitude" for a fermion between an L dyon and an $\overline{L}$ antidyon, defined via the zero mode φ_D of the dyon and the zero mode $\varphi_{\overline{D}}$ (of opposite chirality) of the antidyon,

$$\begin{aligned} \mathbf{T}_{LR} &= \int d^4x \varphi_L^\dagger(x) i(\partial_4 - \mu - i\sigma\cdot\nabla)\varphi_R(x) \\ \mathbf{T}_{RL} &= \int d^4x \varphi_R^\dagger(x) i(\partial_4 - \mu + i\sigma\cdot\nabla)\varphi_L(x), \end{aligned} \tag{6}$$

and similarly for the other components. These matrix elements can be made explicit in the hedgehog gauge,

$$\begin{aligned} \mathbf{T}_{LR} &= e^{i(\alpha_L-\alpha_R)}\mathbf{T}(p) - e^{-i(\alpha_L-\alpha_R)}\mathbf{T}^*(p) \\ \mathbf{T}_{RL} &= e^{i(\alpha_R-\alpha_L)}\mathbf{T}(p) - e^{-i(\alpha_R-\alpha_L)}\mathbf{T}^*(p), \end{aligned} \tag{7}$$

with a complex $\mathbf{T}(p)$ at finite μ,

$$\mathbf{T}(p) = -\frac{1}{2}(\omega_0 + i\mu)(|f_1|^2 - |f_2'|^2) - \mathrm{Re}(f_1 f_2'^*). \tag{8}$$

Here, $f_{1,2} \equiv f_{1,2}(p)$ are the three-dimensional Fourier transforms of $f_1(r) = \alpha_-(r)$ and $f_2(r) = \alpha_-(r)/r$. The transition matrix elements in the string gauge are more involved. Their explicit form is discussed in Appendix A. Throughout, we will make use of the hopping matrix elements in the hedgehog gauge as the numerical difference between the two is small [2] on average as we show in Appendix B.

III. EQUILIBRIUM STATE

The detailed fermionization and bosonization of the instanton liquid model at zero μ was presented in Refs. [1,2,4]. To help set up the notations and understand the logical flow of the new elements of the derivation at finite μ, we summarize the essential steps in Appendix C. With this in mind, to analyze the ground state and the fermionic fluctuations, we bosonize the fermions in (C15) by introducing the identities

$$\begin{aligned} \int D[\Sigma_1]\delta(\psi_f^\dagger(x)\psi_f(x) + 4\Sigma_1(x)) &= \mathbf{1} \\ \int D[\Sigma_2]\delta\left(\frac{1}{2}(\epsilon_{fg}\psi_f^T(x)\psi_g(x) - \mathrm{c.c.}) + 4i\Sigma_2(x)\right) &= \mathbf{1} \end{aligned} \tag{9}$$

and reexponentiating them to obtain

$$\mathcal{Z}_1[T] = \int D[\psi]D[\sigma]D[b]D[\vec{\Sigma}]D[\vec{\lambda}]e^{-S-S_C} \tag{10}$$

with

$$\begin{aligned} -S_C = &\int d^3x i\lambda_1(x)(\psi_f^\dagger(x)\psi_f(x) + 4\Sigma_1(x)) \\ &+ \int d^3x i\lambda_2(x) \\ &\times \left(\frac{1}{2}(\epsilon_{fg}\psi_f^T(x)\psi_g(x) - \mathrm{c.c.}) + 4i\Sigma_2(x)\right). \end{aligned} \tag{11}$$

The ground state is parity even so that $f_{L,M} = f_{\overline{L},\overline{M}}$. By translational invariance, the $SU(2)$ ground state corresponds to constant σ, b, $\vec{\Sigma}$, $\vec{\lambda}$. We will seek the extrema of (10) with finite condensates in the mean-field approximation, i.e.

$$\begin{aligned} \langle\psi_f^\dagger(x)\psi_g(x)\rangle &= -2\delta_{fg}\Sigma_1 \\ \langle\psi_f^T(x)\psi_g(x)\rangle &= -2i\epsilon_{fg}\Sigma_2. \end{aligned} \tag{12}$$

The classical solutions to the constraint equations (C14) are also constant,

$$f_M e^{w_M - w_L} = f_L \left\langle \prod_f \psi_f^\dagger \gamma_+ \psi_f \right\rangle \mathrm{e}^{w_L - w_M}, \tag{13}$$

with

$$\left\langle \prod_f \psi_f^\dagger \gamma_+ \psi_f \right\rangle = (\Sigma_1^2 + \Sigma_2^2) \equiv \vec{\Sigma}^2 \tag{14}$$

and similarly for the antidyons. The expectation values in (13) and (14) are carried in (10) in the mean-field approximation through Wick contractions. Here, we note that both the chiral pairing (Σ_1) and diquark pairing (Σ_2) are of equal strength in the instanton-dyon liquid model. The chief reason is that the pairing mechanism goes solely through the KK- or L-zero modes which are restricted to the affine root of the color group. With this in mind, the solution to (13) is

$$e^{w_M - w_L} = |\vec{\Sigma}|\left(\frac{f_L}{f_M}\right)^{\frac{1}{2}} \tag{15}$$

and similarly for the antidyons.

A. Effective potential

The effective potential $\mathcal{V}$ for constant fields follows from (10) by enforcing the delta-function constraint (C17) before variation (strong constraint) and parity

$$-\mathcal{V}/\mathbb{V}_3 = -4\vec{\lambda}\cdot\vec{\Sigma} + 4\pi f_M v_m (e^{w_M - w_L} + e^{w_{\overline{M}} - w_{\overline{L}}}) + 4\pi f_L v_l \vec{\Sigma}^2 (e^{w_L - w_M} + e^{w_{\overline{L}} - w_{\overline{M}}}) \quad (16)$$

after shifting $\lambda_1 \to i\lambda_1$ for convenience, with $\mathbb{V}_3$ the 3-volume. For fixed holonomies $v_{m,l}$, the constant w's are real by (C14) as all right-hand sides vanish, and the extrema of (16) occur for

$$e^{w_M - w_L} = \pm|\vec{\Sigma}|\sqrt{f_L v_l / f_M v_m}$$
$$e^{w_{\overline{M}} - w_{\overline{L}}} = \pm|\vec{\Sigma}|\sqrt{f_L v_{\overline{l}} / f_M v_{\overline{m}}}. \quad (17)$$

Equations (17) are consistent with (13) only if $v_l = v_m = 1/2$ and $v_{\overline{l}} = v_{\overline{m}} = -1/2$. That is for confining holonomies or a center symmetric ground state. Thus,

$$-\mathcal{V}/\mathbb{V}_3 = \alpha|\vec{\Sigma}| - 4\vec{\lambda}\cdot\vec{\Sigma} \quad (18)$$

with $\alpha = 4\pi\sqrt{f_L f_M}$. We note that for $\vec{\Sigma} = \vec{0}$ there are no solutions to the extrema equations. Since $\vec{\Sigma} = \vec{0}$ means a zero chiral or quark condensate (see below), we conclude that in this model of the dyon-antidyon liquid with light quarks center symmetry is restored only if both the chiral and superconducting condensates vanish.

B. Gap equations

For the vacuum solution, the auxiliary field $\vec{\lambda}$ is also a constant. The fermionic fields in (10) can be integrated out. The result is a new contribution to the potential (18)

$$-\mathcal{V}/\mathbb{V}_3 \to \alpha|\vec{\Sigma}| - 4\vec{\lambda}\cdot\vec{\Sigma} + 2\int \frac{d^3p}{(2\pi)^3} \ln\left((1+\vec{\lambda}^2|\mathbf{T}(p)|^2)^2 - 4\lambda_1^2|\mathrm{Im}\mathbf{T}(p)|^2\right). \quad (19)$$

The saddle point of (19) in $\vec{\Sigma}$ is achieved for parallel vectors

$$\vec{\lambda} = \frac{\alpha}{4}\frac{\vec{\Sigma}}{|\vec{\Sigma}|} \equiv \lambda(\cos\theta, \sin\theta). \quad (20)$$

Inserting (20) into the effective potential (19) yields

$$-\mathcal{V}/\mathbb{V}_3 = 2\int \frac{d^3p}{(2\pi)^3} \times \ln\left((1+\lambda^2|\mathbf{T}(p)|^2)^2 - 4\lambda^2\cos^2\theta|\mathrm{Im}\mathbf{T}(p)|^2\right) \quad (21)$$

with $\lambda = \alpha/4$ now fixed. Equation (21) admits four pairs of discrete extrema satisfying $\delta\mathcal{V}/\delta\theta = 0$ with $\cos\theta = 0, 1$. The extrema carry the pressure per 3-volume

$$-\mathcal{V}_{0,1}/\mathbb{V}_3 = 2\int \frac{d^3p}{(2\pi)^3} \times \ln\left((1+\lambda^2|\mathbf{T}(p)|^2)^2 - 4\lambda^2(0,1)|\mathrm{Im}\mathbf{T}(p)|^2\right). \quad (22)$$

We note $\mathrm{Im}\mathbf{T} = 0$ in (19) for $\mu = 0$. The effective potential has manifest extended flavor $SU_f(4)$ symmetry which is spontaneously broken by the saddle point (20). Since zero μ cannot support the breaking of $U(1)_V$, this phase is characterized by a finite chiral condensate and a zero diquark condensate. For $\mu \neq 0$, we have $\mathrm{Im}\mathbf{T} \neq 0$ in (19). The effective potential loses manifest $SU_f(4)$ symmetry. While the saddle point (20) indicates the possibility of either a chiral or diquark condensate, Eq. (22) shows that the diquark phase is favored by a larger pressure since $\mathcal{V}_0 > \mathcal{V}_1$. The $\mu > 0$ is a superconducting phase of confined and massless baryons.

The chiral and diquark condensates follow from the definitions (12) and the saddle point (20), which are

$$\left(\frac{\langle\overline{q}q\rangle}{T}, -\frac{\langle qq\rangle}{T}\right) = -2(\lambda_1, \lambda_2). \quad (23)$$

For $\mu = 0$, we have $\lambda_2 = 0$ and $\langle\overline{q}q\rangle/T = -\alpha/2$, while for $\mu \neq 0$, we have $\lambda_1 = 0$ and $\langle qq\rangle/T = \alpha/2$, with $\alpha = 4\pi\sqrt{f_L f_M}$ which is independent of μ. This result is in agreement with the general analysis for the QCD-like theories given in Ref. [23] for zero pion mass (see Table 3).

C. Constituent quark mass and scalar gap

In the paired phase with $\lambda_1 = 0$, the momentum-dependent constituent quark mass $M(p)$ can be defined using the determinant (22) to be

$$M(p) = \lambda(\omega_0^2 + p^2)^{\frac{1}{2}}|\mathbf{T}(p)|. \quad (24)$$

In Fig. 1, we show the behavior of the dimensionless mass ratio $(M(p)/\lambda/\omega_0)^2$ as a function of p/ω_0. The oscillatory behavior is a remnant of the Friedel oscillation noted earlier. Using (11)–(12), we note that (24) satisfies

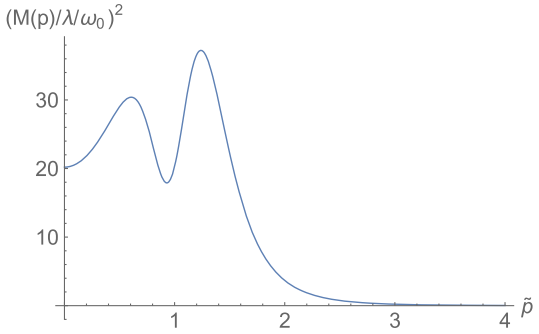

FIG. 1. The squared momentum dependent quark constituent mass $(\omega_0 M(p)/\lambda)^2$ vs $\tilde{p} = p/\omega_0$ for $\mu/\omega_0 = 1$.

$$\int \frac{d^3p}{(2\pi)^3}\frac{M^2(p)}{\omega_0^2+p^2+M^2(p)}=\frac{n_D}{8} \tag{25}$$

with $n_D=8\pi\sqrt{f_L f_M}\Sigma$.

The superconducting mass gap $\Delta_s(0)/2$ can be obtained by fluctuating along the modulus of the paired quark qq. This is achieved through a small and local scalar deformation of the type $\lambda_2(x)\approx\lambda(1+is(x))$, for which the effective action to quadratic order is

$$\mathbf{S}[s]=\frac{2N_f}{2f_s}\int\frac{d^3p}{(2\pi)^3}s(p)\frac{1}{\Delta_s(p)}s(-p). \tag{26}$$

The scalar propagator is ($p_\pm=q\pm\frac{p}{2}$)

$$\frac{1}{\Delta_s(p)}=2\int\frac{d^3q}{(2\pi)^3}\frac{M_+M_-(p_+p_--M_-M_+)}{(p_+^2+M_+^2)(p_-^2+M_-^2)}. \tag{27}$$

Here, we have defined $M_\pm\equiv\lambda|\mathbf{T}(p_\pm)|$, and therefore $\Delta(0)=\Delta_s(0)/\Delta_s'(0)$.

IV. GENERALIZATION TO $SU_c(N_c)\times SU_f(N_f)$

For general N_c with $x=N_f/N_c$, the pairing in (12) involves only those color indices commensurate with the affine root of $SU_c(N_c)$ through their corresponding Kaluza-Klein (KK)- or L-zero modes. This leaves (N_c-2) color directions unbroken. As a result, the nonperurbative contribution to the pressure per unit 3-volume (19) is now changed to

$$\begin{aligned}-\mathcal{V}/\mathbb{V}_3=&\alpha|\vec{\Sigma}|^x-4\vec{\lambda}\cdot\vec{\Sigma}\\&+N_f\int\frac{d^3p}{(2\pi)^3}\\&\times\ln\left((1+\vec{\lambda}^2|\mathbf{T}(p)|^2)^2-4\lambda_1^2|\mathrm{Im}\mathbf{T}(p)|^2\right)\end{aligned} \tag{28}$$

with now $\alpha=4\pi(f_L f_M^{N_c-1})^{\frac{1}{N_c}}$. Remarkably, the fermion loop contribution in (28) is of order $N_fN_c^0$, as it should be for a confining theory with N_c fundamental quarks [24]. The extrema in $\vec{\Sigma}$ still yield parallel vectors

$$\begin{aligned}\vec{\lambda}&=\lambda(\cos\theta,\sin\theta)\\\vec{\Sigma}&=\Sigma(\cos\theta,\sin\theta)\end{aligned} \tag{29}$$

for which (28) simplifies

$$\begin{aligned}-\mathcal{V}/\mathbb{V}_3=&\alpha\Sigma^x-4\lambda\Sigma\\&+N_f\int\frac{d^3p}{(2\pi)^3}\\&\times\ln\left((1+\lambda^2|\mathbf{T}(p)|^2)^2-4\lambda^2\cos^2\theta|\mathrm{Im}\mathbf{T}(p)|^2\right).\end{aligned} \tag{30}$$

The saddle point in Σ gives

$$\lambda=\frac{\alpha}{4}x\Sigma^{x-1}, \tag{31}$$

while the saddle point in θ gives $\cos\theta=0,\,1$. The latter yields the respective pressure per volume,

$$\begin{aligned}-\mathcal{V}_{0,1}/\mathbb{V}_3=&\alpha\left(\frac{4}{\alpha x}\right)^{\frac{x}{x-1}}(1-x)\lambda^{\frac{x}{x-1}}\\&+N_f\ln((1+\lambda^2|\mathbf{T}(p)|^2)^2\\&-4\lambda^2(0,1)|\mathrm{Im}\mathbf{T}(p)|^2).\end{aligned}$$

For $\mu=0$, we have $\mathcal{V}_0=\mathcal{V}_1$, and both the chiral and diquark phases are degenerate. Since the $\mu=0$ phase cannot break $U(1)_V$, the chiral phase with a pion as a Golstone mode is favored. For $\mu>0$, $\mathcal{V}_0>\mathcal{V}_1$, the diquark phase is favored by the largest pressure.

In the diquark phase and for $N_c=3$, the baryonic excitations carry zero triality on average since the phase is still center symmetric. The lightest baryon excitation with zero triality is composed of a massless diquark with color (13) and a constituent quark of color (2) and mass $M(0)$. Here, Eq. (13) refers to the Cartan generator supporting the KK-zero mode at finite μ. As a result, the superconducting phase forms only if

$$\mu>\mu_c=\frac{1}{3}m_B=\frac{1}{3}M(0). \tag{32}$$

From (8), we have

$$M(0)=\lambda\omega_0|\mathbf{T}(0)|=\frac{18\pi^2\lambda}{\omega_0}\frac{(1+\mu^2/\omega_0^2)^{\frac{1}{2}}}{(1+4\mu^2/\omega_0^2)^{\frac{3}{2}}}. \tag{33}$$

Combining (32) and (33) allows for a determination of the critical value λ_c in terms of $\tilde{\mu}_c=\mu_c/\omega_0$,

$$\tilde{\lambda}_c\equiv\frac{\lambda_c}{\omega_0^2}=\frac{\tilde{\mu}_c}{6\pi^2}\frac{(1+4\tilde{\mu}_c^2)^{\frac{3}{2}}}{(1+\tilde{\mu}_c^2)^{\frac{1}{2}}}. \tag{34}$$

Inserting (34) into (24) and (25) yields

$$\frac{n_D}{T^3}=\int d^3x\frac{(\tilde{\lambda}_c\omega_0^2\mathbf{T}(x))^2}{1+(\tilde{\lambda}_c\omega_0^2\mathbf{T}(x))^2} \tag{35}$$

with the hopping transition $\mathbf{T}(x)$ evaluated at $\tilde{\mu}_c$. We have defined

$$n_D=8\pi(f_1..f_{N_c})^{\frac{1}{N_c}}\Sigma^{\frac{N_f}{N_c}}, \tag{36}$$

where each of the N_c dyons carries a fugacity f_i. Note that (36) reduces to the value defined in (25) for $N_c=N_f=2$.

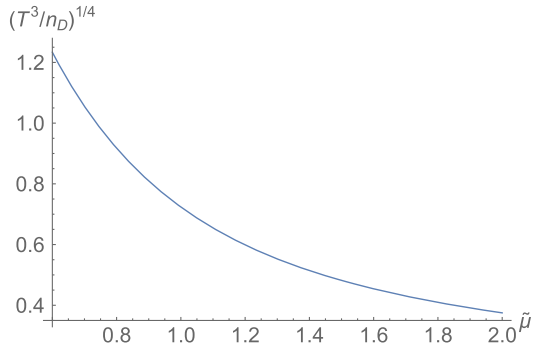

FIG. 2. Critical line $(T^3/n_D)^{\frac{1}{4}} \approx T/\Lambda$ vs $\tilde{\mu} = \mu_c/\omega_0$ for $SU_c(3) \times SU_f(2)$ with n_D defined in (36).

In Fig. 2, we show the critical line for the chemical potential (35), that is $(T^3/n_D)^{\frac{1}{4}} \approx T/\Lambda$ as a function of $\tilde{\mu} = \mu_c/\omega_0$. Here, $\Lambda \approx 200$ MeV is identified with the typical QCD scale [4]. For $T \approx \Lambda$, we have $\mu_c/\Lambda \approx 0.7\pi$, while for $T/\Lambda \approx 0.4$, we have $\mu_c/\Lambda \approx 2\pi$, within the range of validity noted earlier.

In Fig. 3, we sketch the phase diagram for the instanton-dyon ensemble at finite temperature and quark chemical potential for $N_c = 3$ and $N_f = 2$. Below the dashed and lower solid line (blue), the phase is center symmetric and spontaneously breaks chiral symmetry. The phase between the two solid lines (red and blue) is center symmetric and superconducting. The upper (red) line is set by the breaking condition of the superconducting gap, i.e. $T = \Delta_s(0)$ with

$$\frac{1}{\Delta_s(p)} = \frac{x}{1-x}\frac{n_D}{N_c} + \int \frac{d^3q}{(2\pi)^3}\frac{(p_-M_+ + p_+M_-)^2}{(p_+^2+M_+^2)(p_-^2+M_-^2)} \tag{37}$$

which generalizes (27) to any $N_c \neq N_f$. All phase separations (blue) are second order in our mean-field analysis.

The finite μ analysis in the instanton-dyon liquid model is analogous to the 2-color-superconductivity phase in the QCD-like theories [25], as only two out of the three color

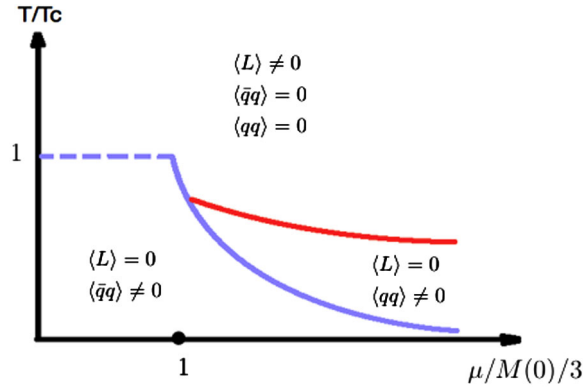

FIG. 3. Sketch of the phase diagram for the instanton-dyon liquid for $SU_c(3) \times SU_f(2)$. See the text.

directions associated to the KK mode (affine root of the Cartan group) are broken. This observation extends to all $N_c > 2$. The instanton-dyon liquid phase does not support a color-flavor-locking phase for $N_c = 3$, since the affine root in $SU_c(3)$ is special and only involves two fixed color directions, say (13). The higher Matsubara modes contribute at the subleading order as we show in Appendix D.

V. CONCLUSIONS

We have extended the mean-field treatment of the $SU(2)$ instanton-dyon model with light quarks in Ref. [1] to finite chemical potential μ. In Euclidean space, finite μ enters through $i\mu$ in the Dirac equation. The antiperiodic KK- or L-dyon zero modes are calculated for the lowest Matsubara frequencies, with the higher modes contributing a subleading order. The delocalization of the zero modes occur only through the KK- or L-dyon zero modes, which implies that the diquark pairing and the chiral pairing have equal strength whatever N_c. Therefore, the instanton-dyon liquid may not support chiral density waves [14]. The diquark phase is favored for $\mu > (1-2/N_c)M(0)$.

ACKNOWLEDGMENTS

This work was supported by the U.S. Department of Energy under Contract No. DE-FG-88ER40388.

APPENDIX A: FERMIONIC HOPPING IN THE STRING GAUGE AT FINITE μ

In this Appendix, we detail the form of the hopping matrix in the string gauge. We will show that the difference with the hopping matrix element in the hedgehog gauge (8) used in the main text is (numerically) small.

We transform the L-zero modes in the hedgehog gauge (2) to the string gauge using the (θ,ϕ) polar parametrization of $\mathbf{S}_\pm$,

$$\begin{aligned}\psi_{\rm L}^{a=1} &= e^{-i\omega_0 x_4}\left(-\sin\frac{\theta}{2}e^{-i\phi}, +\cos\frac{\theta}{2}\right)\alpha_+(r)\\ \psi_{\rm L}^{a=2} &= e^{+i\omega_0 x_4}\left(-\cos\frac{\theta}{2}, -\sin\frac{\theta}{2}e^{+i\phi}\right)\alpha_-(r),\end{aligned} \tag{A1}$$

and similarly for the $\overline{L}$ dyon,

$$\begin{aligned}\psi_{\overline{\rm L}}^{a=1} &= e^{-i\omega_0 x_4}\left(-\cos\frac{\theta}{2}, -\sin\frac{\theta}{2}e^{+i\phi}\right)\alpha_-(r)\\ \psi_{\overline{\rm L}}^{a=2} &= e^{+i\omega_0 x_4}\left(-\sin\frac{\theta}{2}e^{-i\phi}, +\cos\frac{\theta}{2}\right)\alpha_+(r),\end{aligned} \tag{A2}$$

with $\alpha_\pm(r)$ defined in (3). In terms of (A1) and (A2), the hopping matrix element (5) involves the relative angular orientation θ (not to be confused with θ used in the text). It is in general numerically involved.

To gain further insights and simplify physically the numerical analysis, let l_{xy} be the line segment connecting x to y in (5), and let z lie on it. Since the zero modes decay exponentially, the dominant z-contribution to the integral in (5) stems from those z with the smallest $|x-z|+|y-z|$ contribution. Using rotational symmetry, we can set $x=0$ and $y=(r,\theta,0)$ in spherical coordinates. The dominant contributions are from $\theta_{z-x}=\theta$, $\phi_{z-x}=0$, and $\theta_{z-y}=\pi-\theta$, $\phi_{z-y}=-\pi$, which can be viewed as constant in the integral. With this in mind, Eq. (5) in string gauge reads

$$\begin{aligned}-\mathbf{T}^{+}_{LR}(x-y)=&\frac{\omega_0+i\mu}{2}\int d^3z\alpha^*_+(|x-z|)\alpha_+(|y-z|)\\&-\frac{1}{2}\left(1+\frac{\cos^2\theta-\cos\theta}{2}\right)\\&\times\mathrm{Re}\int d^3z\alpha^*_+(|x-z|)\\&\times\frac{\alpha'_+(|y-z|)+\alpha_+(|y-z|)}{|y-z|}.\end{aligned}\tag{A3}$$

In a large ensemble of dyons and antidyons, we have on average $\langle\cos\theta\rangle=0$ and $\langle\cos^2\theta\rangle=\frac{1}{2}$. Thus,

$$\begin{aligned}\mathbf{T}^{+}_{LR}(x-y)=&\frac{\omega_0}{2}\int d^3z\alpha^*_+(|x-z|)\alpha_+(|y-z|)\\&-\frac{5}{8}\mathrm{Re}\int d^3z\alpha^*_+(|x-z|)\\&\times\frac{\alpha'_+(|y-z|)+\alpha_+(|y-z|)}{(|y-z|)}\end{aligned}\tag{A4}$$

in the string gauge. Its Fourier transform is

$$\mathbf{T}(p)\approx-\frac{1}{2}\left((\omega_0+i\mu)|\alpha_+(p)|^2-\frac{5}{4}\mathrm{Re}(\alpha^*_+(p)\tilde{\alpha}_+(p))\right)\tag{A5}$$

with $\tilde{\alpha}(r)=(r\alpha_+(r))'/r$. Equation (A5) is to be compared to (8) in the hedgehog gauge. The dominant contribution in (A5) is due to the first contribution $|\alpha_+|^2$, which is common to both gauge fixing. A similar observation was made in Ref. [2] for the case of $\mu=0$.

APPENDIX B: ESTIMATE OF THE FERMIONIC HOPPING IN THE HEDGEHOG GAUGE AT FINITE μ

In this Appendix, we we will estimate the fermionic hopping matrix element (8) by using the asymptotic form of the L-dyon zero mode at finite μ (2)–(3). Throughout, we will use the dimensionless redefinitions $\mu\to\mu/\omega_0$ and $p\to p/\omega_0$. The normalization in (2) is fixed with

$$\mathbf{C}=\omega_0^{\frac{3}{2}}(8\pi(1+4\mu^2))^{\frac{1}{2}}.\tag{B1}$$

With this in mind, Eq. (8) reads

$$\mathbf{T}(p)=-\frac{\pi}{\omega_0^2}\frac{1}{(1+4\tilde{\mu}^2)}((1+i\mu)\mathbb{F}_1(p)+\mathbb{F}_2(p))\tag{B2}$$

with

$$\begin{aligned}\mathbb{F}_1(p)&=a_1^2(p)-A_1'^2(p)+a_2^2(p)-A_2'^2(p)\\\mathbb{F}_2(p)&=2p(a_1(p)A_1'(p)+a_2(p)A_2'(p))\end{aligned}\tag{B3}$$

$$\begin{aligned}a_1(p)&=\frac{1}{p}\int_0^\infty\sqrt{x}\sin(px)(2\mu\sin(\mu x)+\cos(\mu x))\\a_2(p)&=\frac{1}{p}\int_0^\infty\sqrt{x}\sin(px)(2\mu\cos(\mu x)-\sin(\mu x))\\A_1(p)&=\frac{1}{p}\int_0^\infty\frac{1}{\sqrt{x}}\sin(px)(2\mu\sin(\mu x)+\cos(\mu x))\\A_2(p)&=\frac{1}{p}\int_0^\infty\frac{1}{\sqrt{x}}\sin(px)(2\mu\cos(\mu x)-\sin(\mu x)).\end{aligned}\tag{B4}$$

More explicitly, define

$$\begin{aligned}a(p)&=\frac{\sqrt{2\pi}\sin\left(\frac{3}{2}\tan^{-1}(2p)\right)}{(4p^2+1)^{3/4}}\\b(p)&=\frac{\sqrt{2\pi}\cos\left(\frac{3}{2}\tan^{-1}(2p)\right)}{(4p^2+1)^{3/4}}\\A(p)&=\frac{2\sqrt{\pi}p}{\sqrt{4p^2+1}\sqrt{\sqrt{4p^2+1}+1}}\\B(p)&=\frac{\sqrt{\pi}\sqrt{\sqrt{4p^2+1}+1}}{\sqrt{4p^2+1}}.\end{aligned}\tag{B5}$$

Then, we have

$$\begin{aligned}a_1(p)=&\frac{1}{p}(\mu(b(p-\mu)-b(p+\mu))\\&-\frac{1}{2}(a(p+\mu)+a(p-\mu))\\a_2(p)=&\frac{1}{p}(\mu(a(p-\mu)+a(p+\mu))\\&-\frac{1}{2}(b(p+\mu)-b(p-\mu))\\A_1(p)=&\frac{1}{p}(\mu(B(p-\mu)-B(p+\mu))\\&-\frac{1}{2}(A(p+\mu)+A(p-\mu))\\A_2(p)=&\frac{1}{p}(\mu(A(p-\mu)+A(p+\mu))\\&-\frac{1}{2}(B(p+\mu)-B(p-\mu)),\end{aligned}\tag{B6}$$

We note the momentum averaged hopping strengths

$$\mu=0:\ \int\frac{d^3p}{(2\pi)^3}|\mathbf{T}(p)|^2\approx\frac{4.86}{\omega_0}$$
$$\mu=\omega_0:\ \int\frac{d^3p}{(2\pi)^3}|\mathbf{T}(p)|^2\approx\frac{0.98}{\omega_0},\qquad\text{(B7)}$$

and the typical hopping strengths at zero momentum are

$$\mu=0:\ |\mathbf{T}(0)|^2\approx\frac{307.97}{T^4}$$
$$\mu=\omega_0:\ |\mathbf{T}(0)|^2\approx\frac{0.20}{T^4}.\qquad\text{(B8)}$$

We note the huge reduction in hopping at $\mu=\omega_0$.

APPENDIX C: BOSONIZATION AND FERMIONIZATION

1. Bosonic fields

Following Refs. [1,2,4], the moduli determinants in (1) can be fermionized using four pairs of ghost fields $\chi^\dagger_{L,M}$, $\chi_{L,M}$ for the dyons and four pairs of ghost fields $\chi^\dagger_{\overline{L},\overline{M}}$, $\chi_{\overline{L},\overline{M}}$ for the antidyons. The ensuing Coulomb factors from the determinants are then bosonized using four boson fields $v_{L,M}$, $w_{L,M}$ for the dyons and similarly for the antidyons. The result is

$$\begin{aligned}S_{1F}[\chi,v,w]=-\frac{T}{4\pi}\int d^3x(&|\nabla\chi_L|^2+|\nabla\chi_M|^2\\&+\nabla v_L\cdot\nabla w_L+\nabla v_M\cdot\nabla w_M)\\&+(|\nabla\chi_{\overline{L}}|^2+|\nabla\chi_{\overline{M}}|^2+\nabla v_{\overline{L}}\cdot\nabla w_{\overline{L}}\\&+\nabla v_{\overline{M}}\cdot\nabla w_{\overline{M}}).\end{aligned}\qquad\text{(C1)}$$

For the interaction part $V_{D\overline{D}}$, we note that the pair Coulomb interaction in (1) between the dyons and antidyons can also be bosonized using standard methods [26,27] in terms of σ and b fields. As a result, each dyon species acquires additional fugacity factors such that

$$M:\ e^{-b-i\sigma}\qquad L:\ e^{b+i\sigma}\qquad\overline{M}:\ e^{-b+i\sigma}\qquad\overline{L}:\ e^{b-i\sigma}.\qquad\text{(C2)}$$

Therefore, there is an additional contribution to the free part (C1),

$$S_{2F}[\sigma,b]=\frac{T}{8}\int d^3x(\nabla b\cdot\nabla b+\nabla\sigma\cdot\nabla\sigma),\qquad\text{(C3)}$$

and the interaction part is now

$$\begin{aligned}S_I[v,w,b,\sigma,\chi]=-\int d^3x\,&e^{-b+i\sigma}f_M(4\pi v_m+|\chi_M-\chi_L|^2+v_M-v_L)e^{w_M-w_L}\\&+e^{+b-i\sigma}f_L(4\pi v_l+|\chi_L-\chi_M|^2+v_L-v_M)e^{w_L-w_M}\\&+e^{-b-i\sigma}f_{\overline{M}}(4\pi v_{\overline{m}}+|\chi_{\overline{M}}-\chi_{\overline{L}}|^2+v_{\overline{M}}-v_{\overline{L}})e^{w_{\overline{M}}-w_{\overline{L}}}\\&+e^{+b+i\sigma}f_{\overline{L}}(4\pi v_{\overline{l}}+|\chi_{\overline{L}}-\chi_{\overline{M}}|^2+v_{\overline{L}}-v_{\overline{M}})e^{w_{\overline{L}}-w_{\overline{M}}}\end{aligned}\qquad\text{(C4)}$$

without the fermions. We now show the minimal modifications to (C4) when the fermionic determinantal interaction is present.

2. Fermionic fields

To fermionize the determinant and for simplicity, consider first the case of one flavor and one Matsubara frequency, and define the additional Grassmanians $\chi=(\chi_1^i,\chi_2^j)^T$ with $i,j=1,..,K_{L,\overline{L}}$ and

$$|\det\tilde{\mathbf{T}}|=\int D[\chi]e^{\chi^\dagger\tilde{\mathbf{T}}\chi}.\qquad\text{(C5)}$$

We can rearrange the exponent in (C5) by defining a Grassmanian source $J(x)=(J_1(x),J_2(x))^T$ with

$$J_1(x)=\sum_{i=1}^{K_L}\chi_1^i\delta^3(x-x_{Li})\qquad J_2(x)=\sum_{j=1}^{K_{\overline{L}}}\chi_2^j\delta^3(x-y_{\overline{L}j})\qquad\text{(C6)}$$

and by introducing two additional fermionic fields $\psi(x)=(\psi_1(x),\psi_2(x))^T$. Thus,

$$e^{\chi^\dagger\tilde{\mathbf{T}}\chi}=\frac{\int D[\psi]\exp(-\int\psi^\dagger\tilde{\mathbf{G}}\psi+\int J^\dagger\psi+\int\psi^\dagger J)}{\int dD[\psi]\exp(-\int\psi^\dagger\tilde{\mathbf{G}}\psi)}\qquad\text{(C7)}$$

with $\tilde{\mathbf{G}}$ a 2×2 chiral block matrix,

$$\tilde{\mathbf{G}}=\begin{pmatrix}0&-i\mathbf{G}(x,y)\\-i\mathbf{G}(x,y)&0\end{pmatrix},\qquad\text{(C8)}$$

with entries $\mathbf{TG}=\mathbf{1}$. The Grassmanian source contributions in (C7) generate a string of independent exponents for the L dyons and $\overline{L}$ antidyons,

$$\prod_{i=1}^{K_L}e^{\chi_1^{i\dagger}\psi_1(x_{Li})+\psi_1^\dagger(x_{Li})\chi_1^i}\qquad\prod_{j=1}^{K_{\overline{L}}}e^{\chi_2^{j\dagger}\psi_2(y_{\overline{L}j})+\psi_2^\dagger(y_{\overline{L}j})\chi_2^j}.\qquad\text{(C9)}$$

The Grassmanian integration over the χ_i in each factor in (C9) is now readily done to yield

$$\prod_i [-\psi_1^\dagger \psi_1(x_{Li})] \prod_j [-\psi_2^\dagger \psi_2(y_{\overline{L}j})] \tag{C10}$$

for the L dyons and $\overline{L}$ antidyons. The net effect of the additional fermionic determinant in (1) is to shift the L-dyon and $\overline{L}$-antidyon fugacities in (C4) through

$$\begin{aligned} f_L &\to -f_L \psi_1^\dagger \psi_1 \equiv -f_L \psi^\dagger \gamma_+ \psi \\ f_{\overline{L}} &\to -f_{\overline{L}} \psi_2^\dagger \psi_2 \equiv -f_{\overline{L}} \psi^\dagger \gamma_- \psi, \end{aligned} \tag{C11}$$

where we have now identified the chiralities through $\gamma_\pm = (1 \pm \gamma_5)/2$. The fugacities $f_{M,\overline{M}}$ are left unchanged since they do not develop zero modes.

The result (C11) generalizes to an arbitrary number of flavors N_f and two Matsubara frequencies labeled by i, $j = \pm$ through the substitution

$$\begin{aligned} f_L &\to \prod_{f=1}^{N_f} \prod_{i,j=\pm} \psi_f^\dagger(i_f) \gamma_+ \psi_f(j_f) \delta\left(\sum_f (i_f + j_f) \right) \\ f_{\overline{L}} &\to \prod_{f=1}^{N_f} \prod_{i,j=\pm} \psi_f^\dagger(i_f) \gamma_- \psi_f(j_f) \delta\left(\sum_f (i_f + j_f) \right). \end{aligned} \tag{C12}$$

3. Resolving the constraints

In terms of (C1)–(C4) and the substitution (C11), the dyon-antidyon partition function (1) for finite N_f can be exactly rewritten as an interacting effective field theory in three dimensions,

$$\begin{aligned} \mathcal{Z}_1[T] \equiv \int D[\psi] D[\chi] D[v] D[w] D[\sigma] D[b] \\ \times e^{-S_{1F} - S_{2F} - S_I - S_\psi}, \end{aligned} \tag{C13}$$

with the additional $N_f = 1$ chiral fermionic contribution $S_\psi = \psi^\dagger \tilde{\mathbf{G}} \psi$. Since the effective action in (C13) is linear in the $v_{M,L,\overline{M},\overline{L}}$, the latter integrate to give the following constraints,

$$\begin{aligned} &-\frac{T}{4\pi} \nabla^2 w_M + f_M e^{w_M - w_L} \\ &\quad - f_L \prod_f \psi_f^\dagger \gamma_+ \psi_f e^{w_L - w_M} = \frac{T}{4\pi} \nabla^2 (b - i\sigma) \\ &-\frac{T}{4\pi} \nabla^2 w_L - f_M e^{w_M - w_L} \\ &\quad + f_L \prod_f \psi_f^\dagger \gamma_+ \psi_f e^{w_L - w_M} = 0, \end{aligned} \tag{C14}$$

and similarly for the antidyons with $M, L, \gamma_+ \to \overline{M}, \overline{L}, \gamma_-$. To proceed further, the formal classical solutions to the constraint equations or $w_{M,L}[\sigma, b]$ should be inserted back into the three-dimensional effective action. The result is

$$\mathcal{Z}_1[T] = \int D[\psi] D[\sigma] D[b] e^{-S} \tag{C15}$$

with the three-dimensional effective action

$$\begin{aligned} S = S_F[\sigma, b] + \int d^3x \sum_f \psi_f^\dagger \tilde{\mathbf{G}} \psi_f \\ - 4\pi f_M v_m \int d^3x (e^{w_M - w_L} + e^{w_{\overline{M}} - w_{\overline{L}}}) \\ + 4\pi f_L v_l \int d^3x \prod_f \psi_f^\dagger \gamma_+ \psi_f e^{w_L - w_M} \\ + 4\pi f_{\overline{L}} v_l \int d^3x \prod_f \psi_f^\dagger \gamma_- \psi_f e^{w_{\overline{L}} - w_{\overline{M}}}. \end{aligned} \tag{C16}$$

Here, S_F is S_{2F} in (C3) plus additional contributions resulting from the $w_{M,L}(\sigma, b)$ solutions to the constraint equations (C14) after their insertion back. This procedure for the linearized approximation of the constraint was discussed in Refs. [1,2] for the case without fermions.

APPENDIX D: ALTERNATIVE EFFECTIVE ACTION AT FINITE μ

In this Appendix, we detail an alternative mean-field analysis of the instanton-dyon ensemble at finite T, μ. The construction is more transparent for a diagrammatic interpretation and allows for the use of many-body techniques beyond the mean-field limit. For that, we set $N_f = 2$ and define

$$\langle \psi_f(p) \psi_g^\dagger(-p) \rangle = \delta_{fg} \mathbf{F}_1(p) \tag{D1}$$

$$\langle \psi_f(p) \psi_g^T(-p) \rangle = i\epsilon_{fg} \mathbf{F}_2(p) \tag{D2}$$

with $p = (\vec{p}, \pm\omega_0)$ subsumed. The averaging is assumed over the instanton-dyon ensemble, with

$$\Sigma_{1,2} = \frac{1}{2} \mathrm{Tr} \mathbf{F}_{1,2}. \tag{D3}$$

The trace is carried over the dummy spin indices and momentum. The three-dimensional effective action for the momentum dependent spin matrices $\mathbf{F}_{1,2}$ in the mean-field approximation takes the generic form

$$\begin{aligned} -\Gamma[\mathbf{F}] = \alpha \left(\left(\frac{\mathrm{Tr} \mathbf{F}_1}{2} \right)^2 + \left(\frac{\mathrm{Tr} \mathbf{F}_2}{2} \right)^2 \right)^{\frac{1}{N_c}} \\ + 2\mathrm{Tr} \tilde{\mathbf{G}} \mathbf{F}_1 - \mathrm{Tr} \ln(\mathbf{F}_2^2 + \mathbf{F}_2 \mathbf{F}_1^T \mathbf{F}_2^{-1} \mathbf{F}_1). \end{aligned} \tag{D4}$$

The first contribution is the Hartree-Fock-type contribution to the effective potential after minimizing with respect to $(w_M - w_L)$. The second and third contributions are from the fermionic loop with the fermion propagator evaluated in the mean-field approximation. We note that in the dyon

ensemble both the quark-quark pairing and the quark-antiquark pairing carry equal weight in the Hartree-Fock term. This is not the case for one-gluon exchange or the instanton liquid model where the quark-quark pairing is $1/N_c$ suppressed in comparison to the quark-antiquark pairing. We have checked that the saddle point equations

$$\frac{\delta\Gamma[\mathbf{F}]}{\delta\mathbf{F}_i(p)}=0 \tag{D5}$$

yield the saddle point results in the main text.

APPENDIX E: ZERO MODES FOR ARBITRARY MATSUBARA FREQUENCIES

To discuss the generalized structure of the zero modes for higher Matsubara frequencies, we recall that for the $SU_c(2)$ case the Polyakov line is $L=\cos\pi\nu$. In a dyon with core size and asymptotic A_4 controlled by $\nu\to\nu_n=\nu+n$, there is a tower of zero modes with higher Matsubara frequencies of which (2) and (3) are the lowest ones. To construct them, we first note that each Matsubara mode $\psi\equiv e^{i\omega_m x_4}\tilde{\psi}$ contributes the following to the Dirac equation for $\tilde{\psi}$:

$$(\gamma\cdot D+\gamma_4(-\mu+i\omega_m))\tilde{\psi}=0. \tag{E1}$$

Equation (E1) shows that the zero modes in a BPS dyon follow from the standard ones using the double substitution $\mu\to\mu-i\omega_m$ and $\nu\to\nu_n$. Square integrability for $\omega_m=(2m+1)\omega_0$ requires $|\omega_m|<|\nu_n\omega_0|$. For all m satisfying $|2m+1|<|\nu+n|$, the antiperiodic BPS or M dyon zero modes read explicitly

$$\tilde{\psi}_{m,n,A\alpha}=(\alpha_{1mn}(r)+\alpha_{2mn}(r)\sigma\cdot\hat{r}\epsilon)_{A\alpha} \tag{E2}$$

with

$$\begin{aligned}\alpha_{1,2mn}&=\frac{\chi_{1,2mn}}{\sqrt{2\pi T\nu_n r\sinh(2\pi T\nu_n r)}}\\ \chi_{1,mn}&=-\frac{\phi_m}{\pi\nu_n}\sinh(\phi_m\mathrm{Tr})+\tanh(\pi T\nu_n)\cosh(\phi_m\mathrm{Tr})\\ \chi_{2,mn}&=\mp\left(\frac{\phi_m}{\pi\nu_n}\cosh(\phi_m\mathrm{Tr})-\coth(\pi T\nu_n)\sinh(\phi_m\mathrm{Tr})\right).\end{aligned} \tag{E3}$$

Here, $\phi_m=\omega_m+i\mu/T$, with $-$, $+$ referring to the antiperiodic M- and $\overline{M}$-dyon zero modes, respectively.

For periodic BPS zero modes, we still have (E2) and (E3) but with the substitution $\omega_m\to 2m\omega_0$. Square integrability now requires $|2m|<|\nu+n|$. To construct the antiperiodic KK- or L-dyon zero modes at level n, we first obtain the periodic BPS zero modes with $\nu\to\overline{\nu}$ and $n\to -n$ as detailed above. We then gauge transform them using $e^{\mp i\pi T x_4\sigma\cdot\hat{r}}$ to obtain the antiperiodic KK- or L-dyon zero modes. Therefore, the condition for the existence of antiperiodic L-dyon zero modes at level n, with time dependence $e^{\pm i\omega_0 x_4+i2\pi mTx_4}$ is $|2m|<|\overline{\nu}-n|$.

In summary, the asymptotics of the mode $\psi_{m,n}$ is

$$\psi_{m,n}\to\frac{e^{-(\nu+n-(2m+1))\pi\mathrm{Tr}}}{\sqrt{r}}e^{-i(2m+1)\pi Tx_4}. \tag{E4}$$

Also, for the L dyon at level n, the asymptotics reads

$$\psi^L_{m,n}\to\frac{e^{-(\overline{\nu}+n-2m)\pi\mathrm{Tr}}}{\sqrt{r}}e^{-i(2m+1)\pi Tx_4}. \tag{E5}$$

So, for $n=2m+1$ or $2m$, we have

$$\begin{aligned}\psi_{m,2m+1}&\to\frac{e^{-\nu\pi\mathrm{Tr}}}{\sqrt{r}}e^{-i(2m+1)\pi Tx_4}\\ \psi^L_{m,2m}&\to\frac{e^{-\overline{\nu}\pi\mathrm{Tr}}}{\sqrt{r}}e^{-i(2m+1)\pi Tx_4}.\end{aligned} \tag{E6}$$

For example, at $n=1$, all the M zero modes at ω_0 decay as $e^{-\pi T\nu r}/\sqrt{r}$, which is the same as the L zero mode at $n=0$. Thus, even though they carry higher Matsubara frequencies, their asymptotics are the same compared with those modes with $n=0$. However, since they are assiociated with dyons with larger action or small fugacity, they are always suppressed. For example, the induced effective contribution to the action which includes the modes at $n=1$ and $m=0$ is

$$\begin{aligned}&\sum_{i=1}^{N_c-1}f_{i,n=0}e^{w_i-w_{i+1}}+f_{N_c,n=0}\prod_f\psi^\dagger_f\psi_f e^{w_{N_c}-w_1}\\ &\quad+\sum_{i=1}^{N_c-1}f_{i,n=1}\prod_f\psi^\dagger_{f,1}\psi_{f,1}e^{w^1_i-w^1_{i+1}}.\end{aligned} \tag{E7}$$

The last contribution is due to the higher Matsubara modes. However, this contribution is exponentially suppressed compared to the first two contributions we have retained in the text, since

$$f_{i,n=1}/f_{i,n=0}=e^{-\frac{16\pi^2}{g^2}}. \tag{E8}$$

[1] Y. Liu, E. Shuryak, and I. Zahed, Phys. Rev. D **92**, 085006 (2015).

[2] Y. Liu, E. Shuryak, and I. Zahed, Phys. Rev. D **92**, 085007 (2015).

[3] T. C. Kraan and P. van Baal, Nucl. Phys. **B533**, 627 (1998); Phys. Lett. B **435**, 389 (1998); K. M. Lee and C. h. Lu, Phys. Rev. D **58**, 025011 (1998).

[4] D. Diakonov and V. Petrov, Phys. Rev. D **76**, 056001 (2007); **76**, 056001 (2007); AIP Conf. Proc. **1343**, 69 (2011); D. Diakonov, arXiv:1012.2296.

[5] D. Diakonov, N. Gromov, V. Petrov, and S. Slizovskiy, Phys. Rev. D **70**, 036003 (2004).

[6] R. Larsen and E. Shuryak, Nucl. Phys. **A950**, 110 (2016).

[7] A. R. Zhitnitsky, arXiv:hep-ph/0601057; S. Jaimungal and A. R. Zhitnitsky, arXiv:hep-ph/9905540; A. Parnachev and A. R. Zhitnitsky, Phys. Rev. D **78**, 125002 (2008); A. R. Zhitnitsky, Nucl. Phys. **A921**, 1 (2014).

[8] M. Unsal and L. G. Yaffe, Phys. Rev. D **78**, 065035 (2008); M. Unsal, Phys. Rev. D **80**, 065001 (2009); E. Poppitz, T. Schafer, and M. Unsal, J. High Energy Phys. 10 (2012) 115; E. Poppitz and M. Unsal, J. High Energy Phys. 07 (2011) 082; E. Poppitz, T. Schafer, and M. Unsal, J. High Energy Phys. 03 (2013) 087.

[9] M. N. Chernodub, T. C. Kraan, and P. van Baal, Nucl. Phys. B, Proc. Suppl. **83**, 556 (2000).

[10] E. Shuryak and T. Sulejmanpasic, Phys. Rev. D **86**, 036001 (2012); Phys. Lett. B **726**, 257 (2013).

[11] P. Faccioli and E. Shuryak, Phys. Rev. D **87**, 074009 (2013).

[12] E. Poppitz and T. Sulejmanpasic, J. High Energy Phys. 09 (2013) 128.

[13] R. Rapp, T. Schfer, E. V. Shuryak, and M. Velkovsky, Phys. Rev. Lett. **81**, 53 (1998); Ann. Phys. (N.Y.) **280**, 35 (2000); M. G. Alford, K. Rajagopal, and F. Wilczek, Phys. Lett. B **422**, 247 (1998); M. G. Alford, K. Rajagopal, and F. Wilczek, Nucl. Phys. **B537**, 443 (1999).

[14] E. Shuster and D. T. Son, Nucl. Phys. **B573**, 434 (2000); B. Y. Park, M. Rho, A. Wirzba, and I. Zahed, Phys. Rev. D **62**, 034015 (2000).

[15] A. S. Goldhaber and N. S. Manton, Phys. Lett. B **198**, 231 (1987); L. Castillejo, P. S. J. Jones, A. D. Jackson, J. J. M. Verbaarschot, and A. Jackson, Nucl. Phys. **A501**, 801 (1989).

[16] M. Rho, S. J. Sin, and I. Zahed, Phys. Lett. B **689**, 23 (2010); V. Kaplunovsky, D. Melnikov, and J. Sonnenschein, Mod. Phys. Lett. B **29**, 1540052 (2015).

[17] C. Ratti, S. Roessner, M. A. Thaler, and W. Weise, Eur. Phys. J. C **49**, 213 (2007); S. Roessner, C. Ratti, and W. Weise, Phys. Rev. D **75**, 034007 (2007); H. Abuki and K. Fukushima, Phys. Lett. B **676**, 57 (2009); D. Scheffler, M. Buballa, and J. Wambach, Acta Phys. Pol. B Proc. Suppl. **5**, 971 (2012).

[18] I. Barbour, N. E. Behilil, E. Dagotto, F. Karsch, A. Moreo, M. Stone, and H. W. Wyld, Nucl. Phys. **B275**, 296 (1986); J. Han and M. A. Stephanov, Phys. Rev. D **78**, 054507 (2008).

[19] Z. Fodor, S. D. Katz, and C. Schmidt, J. High Energy Phys. 03 (2007) 121.

[20] V. G. Bornyakov, E.-M. Ilgenfritz, B. V. Martemyanov, and M. Muller-Preussker, Phys. Rev. D **91**, 074505 (2015); arXiv:1512.03217.

[21] T. Schafer and E. V. Shuryak, Rev. Mod. Phys. **70**, 323 (1998); D. Diakonov, Prog. Part. Nucl. Phys. **51**, 173 (2003); M. A. Nowak, M. Rho, and I. Zahed, *Chiral Nuclear Dynamics*, (World Scientific, Singapore, 1996), p. 528.

[22] F. Bruckmann, R. Rodl, and T. Sulejmanpasic, Phys. Rev. D **88**, 054501 (2013).

[23] J. B. Kogut, M. A. Stephanov, D. Toublan, J. J. M. Verbaarschot, and A. Zhitnitsky, Nucl. Phys. **B582**, 477 (2000).

[24] T. H. Hansson and I. Zahed, Phys. Lett. B **309**, 385 (1993).

[25] R. Rapp, T. Schfer, E. V. Shuryak, and M. Velkovsky, Phys. Rev. Lett. **81**, 53 (1998); M. G. Alford, K. Rajagopal, and F. Wilczek, Phys. Lett. B **422**, 247 (1998); K. Rajagopal and F. Wilczek, *At the Frontier of Particle Physics*, edited by M. Shifman (World Scientific, Singapore, 2001), Vol. 3, p. 2061.

[26] A. M. Polyakov, Nucl. Phys. **B120**, 429 (1977).

[27] M. Kacir, M. Prakash, and I. Zahed, Acta Phys. Polon. B **30**, 287 (1999).

[28] Y. Liu, E. Shuryak, and I. Zahed, following paper, Phys. Rev. D **94**, 105012 (2016).